ACS OMEGA

http://pubs.acs.org/journal/acsodf

Article

Application of Rheo-optic In Situ Measurement Technology to Study Waxy Crude Oil Rheology

Hang Dong, RunZe Ma, Jian Zhao,* Xiangrui Xi, and Zhihua Wang

Cite This: *ACS Omega* 2022, 7, 17948−17962

Read Online

ACCESS | Metrics & More | Article Recommendations | Supporting Information

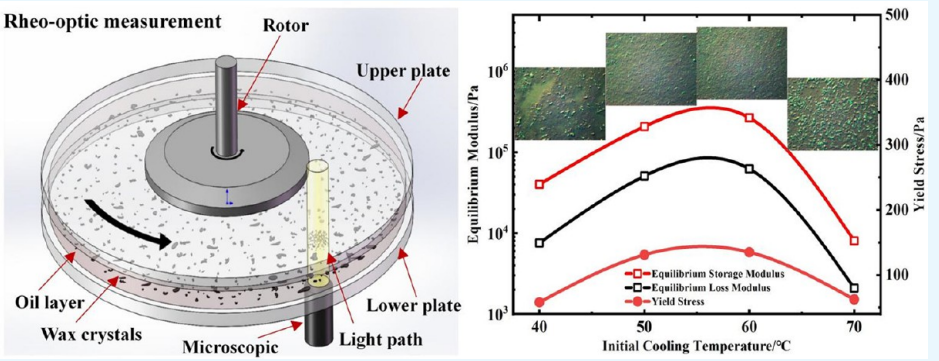

ABSTRACT: The micromechanism of waxy crude oil gelling is the interaction between wax crystals to form a certain intensity flocculation structure, which significantly increases the cost of production and transmission. In this paper, rheo-optic in situ measurement technology is applied to the rheological study of waxy crude oil for the first time and also to the rheological response of typical waxy crude oil to thermal history, the micromechanism of shear-thinning, and the dynamic behavior of wax crystal. Through the new experimental technique and analysis method, it is found that two types of wax crystals can be formed under certain thermal historical conditions, which have opposite performances in microscopic morphology, mechanic properties, and flocculation tendency, and the change of its proportion in crude oil is the root cause of the initial cooling temperature affecting the fluency of waxed crude oil. It was found that the microscopic behavior of waxy crude oil with the increase of shear rate went through the following whole process: the waxy crude oil system changes from static to dynamic, the wax crystal flocculation network undergoes deformation, cracks, and ruptures, and wax crystal aggregates break, small aggregates orient along the flow field, and small aggregates continues to deform and break. When the shear rate is below 5 s^{-1}, the crack of the flocculation structure plays a leading role. It is only after the shear rate exceeds 5 s^{-1} that the deformation of the wax crystal and its flocs begins to function. Furthermore, according to the microscopic images of the wax crystals motion sequence, the micromorphology of different types of flocs and the dynamic behaviors under shearing are systematically analyzed by dynamic micro-object capture technology.

1. INTRODUCTION

The rheological properties of crude oil refer to relationships between flow and deformation under forces, which can change considerably under different temperature and pressure conditions.[1] Research on crude oil rheological properties is important for the determination of safety parameters and operational adjustments during storage and transportation.[2−4] In general, properties of crude oil, such as high wax appearance temperature (WAT), high pour point, and high wax content, can contribute to accidents that reduce oil transportation efficiency and block pipelines. Therefore, heat treatment or the addition of pour point depressants (PPDs) is generally used to improve the rheological properties of crude oil, but high production costs are a disadvantage.[5−7] Consequently, the study of waxy crude oil is very important to ensure the stable and efficient supply of petroleum.[8,9]

Many studies show that the root causes of the deterioration of the low-temperature rheological properties of waxy crude oil are the crystallization and precipitation of wax and the gradual formation of a three-dimensional network structure, which result in the transition from a sol to a structural gel.[10−12] Much research has been conducted on waxy crude oil rheological properties,[13−17] wax crystal morphology,[18,19] and mechanical analysis[20,21,27] and imaging experiments[22−26] to study microscopic and macroscopic aspects of the complex rheological

Received: March 2, 2022
Accepted: May 4, 2022
Published: May 19, 2022

Table 1. Basic Properties of the Crude Oil Sample

properties	value	experimental method	equipment
density at 20 °C (kg/m^3)	832.6	U-tube oscillation	densimeter (4500M, Anton Paar)
pour point (°C)	21	ASTM D5853-11	crude oil freezing point and pour point tester (DSY-006B)
WAT (°C)	48	PLM	polarized light microscopy (PLM) imaging system (Nikon LV100NPOL)
wax melting point (°C)	60.3	PLM	polarized light microscopy imaging system (Nikon LV100NPOL)
wax content (wt %)	16.34	DSC	DSC (differential scanning calorimetry) (TA-Q2000)
saturated hydrocarbon content (wt %)	65.8	SY/T 5119-2016	column separation
aromatic hydrocarbons content (wt %)	18.0		
resins (wt %)	11.8		
asphaltene content (wt %)	4.4		
viscosity at 50 °C (mPa·s)	12.342	SY/T 0520-2008	MCR 702 (Anton Paar)

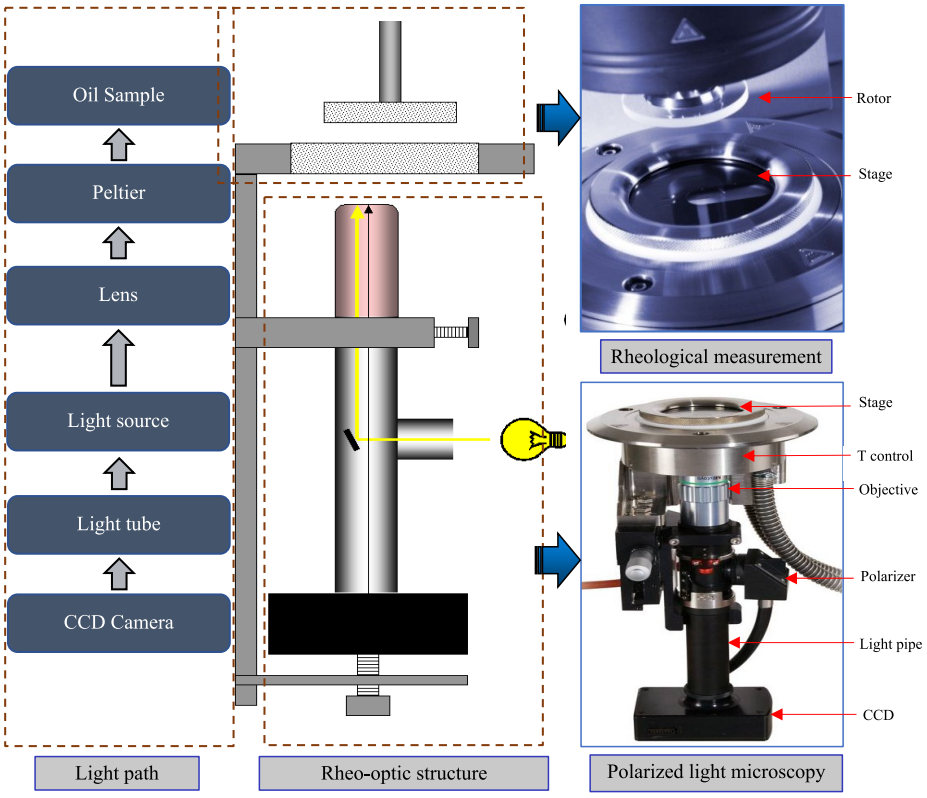

Figure 1. Schematic diagram of the in situ synchronous rheo-optic measurement system. Photograph courtesy Anton Paar. Copyright 2021.

properties of waxy crude oil and the mechanism of wax crystallization.[27−30] At present, useful results have been achieved, but several key issues need to be addressed. (a) Many scholars have published microimages of wax crystal morphology. However, especially under specific conditions or the action of PPDs, the development of wax crystal morphology is complex, and its contribution to changes in system fluidity is not completely clear.[31−35] (b) An increasing number of scholars have observed that, in addition to the influence of wax crystal morphology, the interaction between wax crystals is critical in determining macroscopic rheological properties of oil.[36−39] However, current research methods cannot effectively explore these properties and mechanics performance. (c) Scholars pay much attention to the simultaneous measurement of waxy crude oil rheology and microstructure. However, current research still uses two types of instruments, rheometers and polarizing microscopes. The differences between the two measurement environments and experimental processes present a challenge to obtaining macro- and microscale results. Simultaneous measurements of rheological properties and in situ microscopic observations can effectively overcome this problem. (d) At present, there is no approach to investigate the mechanical properties and transmission behavior of network structures formed by wax crystals.

The dynamic response of network structures under external forces directly determines the macromechanical behavior of waxy crude oil. In particular, beyond the initial yield event, waxy crude oil exhibits rheomalaxis behavior, in which differential imposed deformation causes irreversible changes in the structural state.[40−42] However, the current macro-imaging methods cannot strongly support this research. If it is possible to explore the correlation between wax crystal particles and network structures, then the results may further explain the mechanism of the macromechanical properties of waxy crude oil in terms of the complex dynamic response of the network structure. Then, we can surpass the limitations of conventional macro-image research and make discoveries by

https://doi.org/10.1021/acsomega.2c01251
ACS Omega 2022, 7, 17948−17962

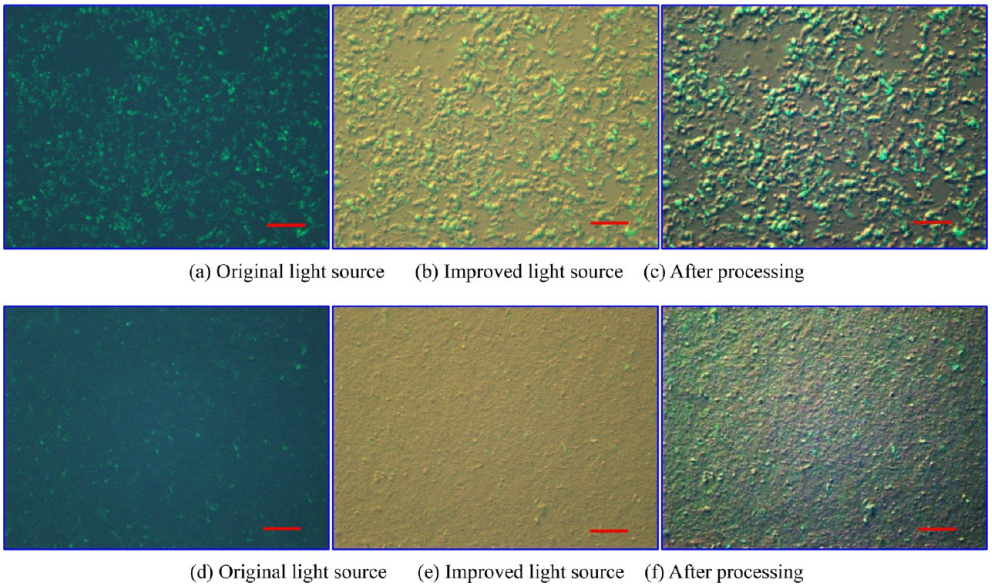

Figure 2. Comparison of images obtained with the original light source (a, d), images obtained with the improved light source (b, e), and processed images (c, f) (scale 50 μm).

studying waxy crude oil rheological properties from a microscopic point of view. This approach is commonly used in particle matter mechanics to explore macromechanical properties and micromechanisms of particle systems.[43,44] To solve the above problems, new experimental methods are needed. Simultaneous in situ rheo-optic measurement technology has been widely used in studies of suspensions and blood to achieve important results. Therefore, by obtaining micrometric performance parameters, microstructures, and dynamic behavior of complex systems, in situ rheo-optic observation systems provide a new means for solving the above problems. Therefore, for the first time, this paper introduces simultaneous in situ rheo-optic measurement technology for the rheological study of waxy crude oil. With an improved light source, more comprehensive and accurate observations of the morphology of wax crystals can be made in situ and associated with macroscopic rheological properties.

In addition, simultaneous microscopic observations can investigate changes in the microstructure and appearance of wax crystals in crude oil under the action of shear and other external forces and obtain the mechanical structural properties of wax particles. The dynamic response of the wax crystal network to external force can include deformation, crushing, and recombination, and this dynamic response can be associated with mechanical parameters obtained simultaneously. In this study, an MCR 702 modular rheometer (Anton Parr) was used to measure macro- and microscale performance of waxy crude oil, including the effect of initial cooling temperature on viscoelasticity, the microscale mechanism of shear thinning, the dynamic response of the structure of wax crystal networks, and the dynamic behavior of wax particles.

2. EXPERIMENTAL SECTION

2.1. Experimental Materials. The experimental oil sample was taken from the Hulunbuir Oilfield in China, a typical waxy crude oil. Before the experiment, the oil sample is divided into sealed reagent bottles and pretreated to eliminate the influence of thermal history and shear history on the physical properties of the oil sample, thereby improving the repeatability and accuracy of subsequent experimental results. Prior to experimental tests, the samples were placed in water bath to be heated at 80 °C for 2 h. Then the samples were naturally cooled to the room temperature and kept for at least 48 h. For the oil sample after pretreatment, its fundamental physical and chemical properties were tested first, and the results are shown in Table 1.

2.2. Experimental Instrument. The instrument used in the experiment is an MCR 702 modular dual-drive rheometer from Anton Paar Company. It is equipped with a polarized light microscopy imaging system, which can simultaneously observe the evolution of wax crystal morphology and dynamic behavior in situ while applying shear to waxy crude oil for rheological measurements. Figure 1 is a schematic diagram of the partial structure of this measurement system.

The rheology measurement used a 43 mm diameter parallel plate measurement system made of transparent quartz glass. A motorhead drives the measuring rotor on the rheometer. A microscope, light source, and regulator are integrated with the lower part of the stage. When the rotor drives the oil sample to flow, the light source illuminates the sample vertically from below. At the same time, images or videos of the microscopic morphology and dynamic behavior of the wax crystals in the oil sample are collected by the microscope in real-time, and a charged-coupled device (CCD) camera (Lumenera) performs video and image collection. The microscope uses a 20× magnification objective lens with a focal length of 30.9 mm and a lens depth of 1.6 μm with optical compensation; it can achieve a resolution of 0.7 μm. The field of view is 440 μm × 330 μm. The microscope is equipped with a 150 W LED light source that provides high-intensity light from one side. The temperature control unit of the experimental system consists of two parts, both of which use the Peltier temperature control principle. The temperature can be changed according to an established procedure. The temperature control range is −20 to +200 °C. In this paper, this experimental system is used to simultaneously make in situ rheological measurements and microscopic observations to study the microstructure evolution and dynamic behavior of wax crystals in waxy crude oil.

https://doi.org/10.1021/acsomega.2c01251
ACS Omega 2022, 7, 17948−17962

Although this experimental system has been used to achieve good results for colloidal suspensions and emulsions,[45,46] no scholars have applied it to the study of waxy crude oil. This is mainly due to the poor light transmission of waxy crude oil, the insufficient reflection of light by wax crystals, and the limited ability to observe wax crystals. Now, the light source of the instrument is improved. In addition to using the light source that comes with the instrument to irradiate the sample vertically from below, a fixed LED light source is applied to the upper part of the sample. By optimizing the adjustment of the fixed LED, the two light sources are superimposed to obtain a microscopic image of the wax crystals in different liquid layers in the sample as well as the locations of wax crystals in a liquid layer. This improves the accuracy of the morphological observations of wax crystals and provides more information about their morphological structure. In addition, to improve the quality of the microimages, the auto level method is used to remove haze,[47] the linear processing of pixels improves brightness and contrast, and the median filtering method removes noise.[48] Figure 2 shows two examples of images of wax crystals taken before and after improving the light source as well as the results of image processing.

The light source and image processing can improve the veracity of the microimages and provide more accurate information about wax crystal morphology. In particular, under certain conditions, wax crystals formed in crude oil do not strongly reflect light (Figure 2d), or some wax crystals in the field of view reflect a very small amount of light (Figure 2a). With only the original light source, only a few wax crystals with good reflective properties or only part of the structural image with a strong wax crystal luminescence effect can be observed. Improving the light source reveals more wax crystals (Figure 2b), the actual number of wax crystals and a complete picture of their characteristics (Figure 2b). Further optimization of the image processing technology can improve the recognition accuracy of the edge and structure of wax crystals (Figure 2, parts c and f), which inevitably improves the quantitative accuracy of the microscale features and parameters of wax crystals.

2.3. Verification of Experimental Results. *2.3.1. Microscopic Observations.* Since this is the first time that this measurement system is applied to the study of waxy crude oil, it is necessary to evaluate the accuracy of the experimental results. First, the morphology of wax crystals formed by cooling the same oil sample is observed with a conventional polarizing microscope (Nikon ECLIPSE LV100NPOL), and the image is quantitatively analyzed. The observations with the conventional microscope and rheo-optic instrument are compared in Figure 3. The particle size distributions of the wax crystals were quantitatively obtained with the two observation methods as shown in Figure 3.

As seen from Figure 3, due to the different limitations of the structure, light source, and observation field of view of the two microscopes, there appear to be some differences in the wax crystal morphologies observed with the two instruments. The contrast between wax crystals and crude oil is more important in conventional observation methods, and the contrast is evident in the images. The difference between wax crystals and crude oil is more obvious in the conventional observation method. The contrast in the image is noticeable, the boundary profile of the wax crystal observed by the rheo-optic instrument is clearer, and the identification of the wax crystal morphology is more accurate than in the images obtained with the conventional microscope. However, the size distributions obtained by the two instruments are the same, and the peak in each particle size distribution is at approximately 3 μm. The rheo-optic instrument identifies more small wax crystals and fewer large wax crystals than does the conventional microscope. This is related to the ability of the rheo-optic instrument to recognize boundary contours of wax crystals with greater accuracy that the conventional microscope. With the rheo-optic instrument, it is less likely that two adjacent wax crystals are recognized as a large wax crystal, and the apparent proportion of tiny wax crystals is higher than that obtained with the conventional microscope.

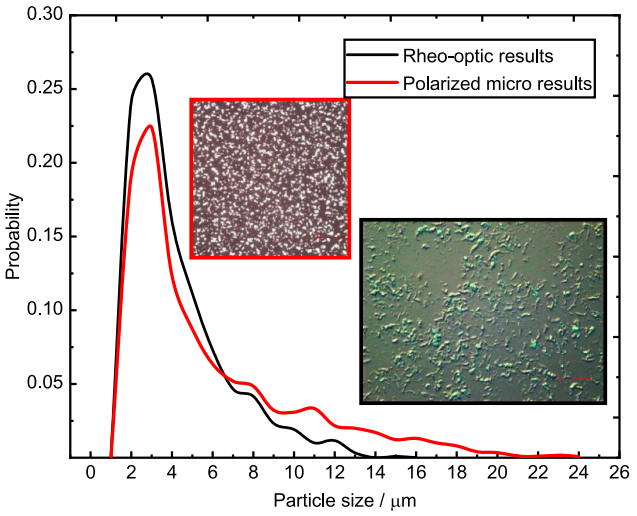

Figure 3. Quantitative wax particle size distributions from different observation methods

2.3.2. Rheological Results. Next, the viscosity of a standard oil at constant 20 s^{-1} shear rate was measured using the rheo-optic instrument, and the results were compared with the standard value, as shown in Figure 4a. The rheological data are stable and accurate, with a 13.1% relative deviation from the standard value. However, unlike a standard oil, waxy crude oil below the WAT temperature is a multiphase system with nonlinear and random microstructure that makes it more challenging to accurately measure its rheological properties. The small amplitude oscillatory shear (SAOS) test was conducted using the waxy crude oil in the plate−plate test module and the rheo-optic module of the MCR 702 rheometer under the same constant temperature conditions. The relationship between the measured balance storage module and the initial cooling temperature is shown in Figure 4b. Although the relative deviation of the two measurements increases from 13.9 to 19.52%, considering the complexity of the structure of waxy crude oil and the same trend in both measurement results, the rheo-optic results show the effect of different experimental conditions on waxy crude oil rheological properties. In addition, considering the advantages of simultaneous in situ measurements, the above error does not affect the effectiveness of the rheo-optic instrument for studying the rheological properties and microscale mechanism of waxy crude oil. Furthermore, so as to ensure the validity of experimental results, the experiments under each condition were repeated at least twice with the relative deviation falling in 15%. And then the average experimental results were used for analysis and discussion.

https://doi.org/10.1021/acsomega.2c01251
ACS Omega 2022, 7, 17948−17962

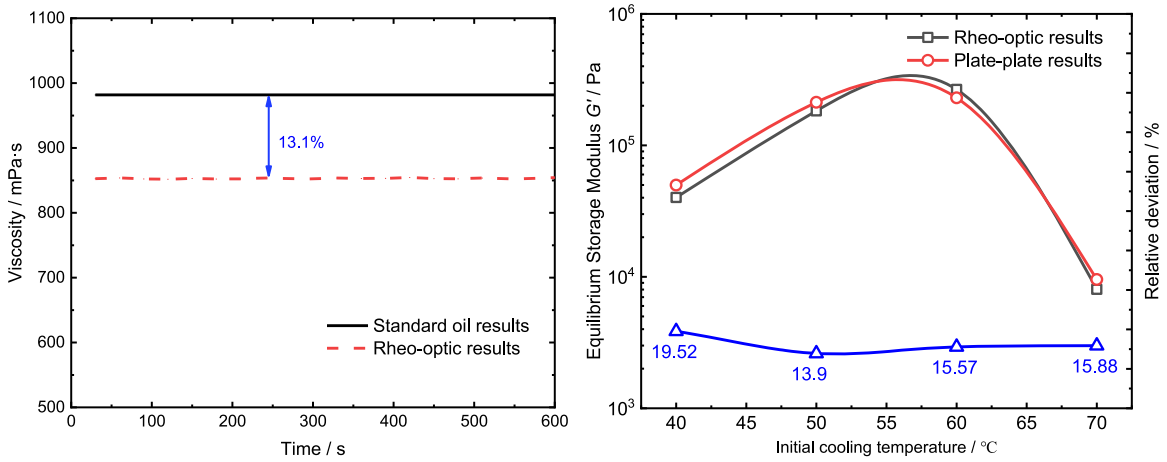

Figure 4. Verification of rheological measurements: (a) waxy oil and standard oil; (b) rheo-optic and plate−plate.

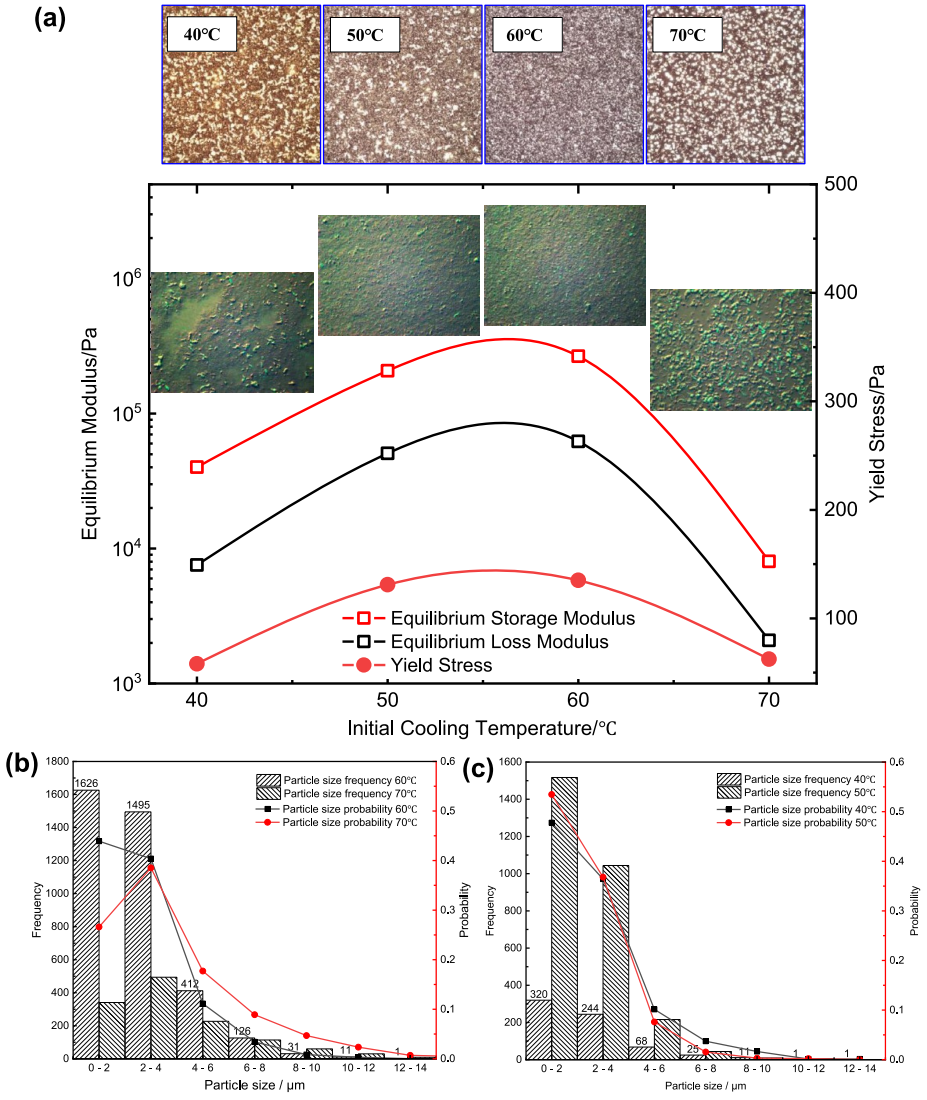

Figure 5. Microscopic and wax particle distributions results: (a) microscopic results of different methods; (b, c) wax particle distributions under different initial cooling temperatures.

3. RESULTS AND DISCUSSION

3.1. Effect of Initial Cooling Temperature on the Viscoelastic Behavior and Gelation of Waxy Crude Oil.

Prior studies have reported on the effect of initial cooling temperature on the rheological properties of waxy crude oil. The effect is attributed to differences in the presence and activity of asphalt at various heating temperatures, which

https://doi.org/10.1021/acsomega.2c01251
ACS Omega 2022, 7, 17948−17962

influence the cooling and growth of wax crystals and changes the appearance of wax crystals. Therefore, the mechanism of the effect of initial cooling temperature can be understood in terms of the microstructure and morphology of wax crystals and, thus, the rheological properties of waxy crude oil. However, there is no systematic understanding of the influence of the initial cooling temperature on the details of changes in morphology and the underlying mechanism of the effects on rheological properties. Applying in situ rheo-optic measurement technology, we can observe the changes in the microstructure of wax crystals while obtaining viscoelastic data for waxy crude oil. This makes it possible to obtain more comprehensive and accurate microscopic information about wax crystals and reveal the microscale mechanism and fundamental mechanical properties of wax crystals that affect the viscoelasticity of waxy crude oil at the initial cooling temperature.

In this experiment, Hulunbel crude oil was used as an experimental oil sample, and it was cooled from an initial temperature of 70, 60, 50, or 40 °C to 20 °C, respectively. The 40 min SAOS test was then performed at constant temperature. The obtained equilibrium storage modulus and corresponding microimages are shown in the figure below. Large amplitude oscillatory shear (LAOS) measurements were used to obtain the yield stress, also shown in the figure. At the same time, the polarizing microscope was used to observe the microscopic morphology of wax crystals that formed after cooling from different initial cooling temperatures; the results are shown in Figure 5.

As seen from the microscopic images in Figure 5, there are observable differences in the wax crystal structure formed by the cooling process from different initial cooling temperatures. With increasing initial cooling temperature, there is a trend in the change of the wax crystal structure. When the initial cooling temperature is 60 °C, many small wax crystals form, and they do not strongly reflect light. These wax crystals are closely arranged in crude oil and cover almost the entire field of view. Compared with the observations in polarizing microscopy, the results in rheo-optic measurement are more conducive to identifying the small but dense wax particles because of the enhanced light source. There is a larger number of wax crystals distributed within a larger field of view. According to the literature, the interaction forces between wax crystals are mainly van der Waals. When wax crystals are closer together, have larger surfaces areas, or have stronger attractive interactions, it is easier to form a large-scale flocculated structure. For this kind of wax crystal structure formed gelation has the most viscoelastic property and highest yield value. In contrast, the wax crystals formed by cooling from an initial cooling temperature of 70 °C are larger with smaller surface areas, and they reflect light more strongly. The wax crystals are widely spaced and have weak attractions; as a result, the gelation state waxy crude oil formed under 70 °C has the least viscoelastic property and lowest yield value. The distribution of wax grain size in Figure 5a also prove this point, as shown in Figure 5, parts b and c. At the initial cooling temperature of 60 °C, the number and proportion of small wax crystals with a particle size of less than 4 μm are much higher than those at 70 °C. The opposite trends are observed for larger particle sizes, i.e., when the wax particle size exceeds 4 μm. Consequently, the wax crystal structure differs fundamentally when it forms at different initial cooling temperatures, which leads to a large disparity in the viscoelasticity of the crude oil system. Wax crystals formed at the initial temperature of 70 °C are referred to as Type I, and the other wax crystals are referred to as Type II. The viscosities of the gels formed by cooling from temperatures of 40 and 50 °C are between those of the above two cases. The lower the temperature is, the smaller the modulus of the system. Although the yield value at initial temperature of 40 °C is very close to that at 70 °C, it is the lowest and has a deviation from the viscoelastic results. This may caused by randomness and complexity of wax crystal structure under SAOS test. In addition, Figure 5a shows that the wax crystals formed at the initial cooling temperatures of 50 and 40 °C contain both Type I and Type II wax crystals. With the initial cooling temperature is lower, the proportion of Type I wax crystals is higher, and the proportion of Type II wax crystals is lower, and the structure consists mainly of Type II wax crystals with embedded Type I wax crystals. The wax particle size distributions in Figure 5c also show that the number and proportion of small wax crystals (especially those with a diameter less than 2 μm) are fewer at 40 °C than in the wax crystals generated by an initial cooling temperature of 50 °C, which is the opposite of the large wax crystals. In contrast, the two microscale observation methods are similar in accuracy and ability to recognize Type I wax crystals. However, for Type II wax crystals, due to their specific structural and morphological characteristics, their reflectivity is not as good as that of Type I wax crystals. The new in situ rheo-optic measurement method can better identify Type II wax crystals, obtain more comprehensive information about wax crystals in crude oil, and improve the accuracy of the description of the wax crystal morphological structure in comparison to the conventional microscopy method. In addition, Figure 5 further illustrates that with the change in wax crystal structure, the interactions between wax crystals and the flocculation tendency also change. As a result, the viscoelasticity parameters gradually decreases when the initial cooling temperature decreases from 60 to 40 °C.

Thus, Type I wax crystals help to reduce the stickiness and elasticity of the system, while Type II wax crystals increase the system's viscoelasticity. These two factors jointly determine the system's viscoelasticity performance. It is thought that this is related to the role of asphalt in crude oil because of the essential difference in the wax crystal structure formed at different initial cooling temperatures. When the initial cooling temperature is greater than 70 °C, not only do wax crystals fully dissolve, but asphalt can fully disperse. Then, asphalt interacts with wax crystals during the subsequent cooling process, plays the role of a natural PPD and improves the wax crystal structure, which promotes the formation of Type I wax crystals in the system. However, although the wax crystals can fully dissolve when the initial cooling temperature is 60 °C, asphalt does not fully disperse and activate. Therefore, it cannot improve wax crystal structure during the cooling process, which results in the formation of Type II wax crystals. Because all oil samples underwent a heat treatment process at 80 °C before the experimental procedure, the wax crystal structure improved, and Type I wax crystals formed after cooling. Under this premise, when the heating temperature is lower, more Type I wax crystals remain in the system, and the system is more fluid. This results in a larger proportion of Type I than Type II wax crystals at an initial cooling temperature of 40 °C. Because the wax melting point of the experimental oil sample is 60.3 °C, fewer Type I was crystals remain after heating at temperatures closer to the wax melting point.

https://doi.org/10.1021/acsomega.2c01251
ACS Omega 2022, 7, 17948−17962

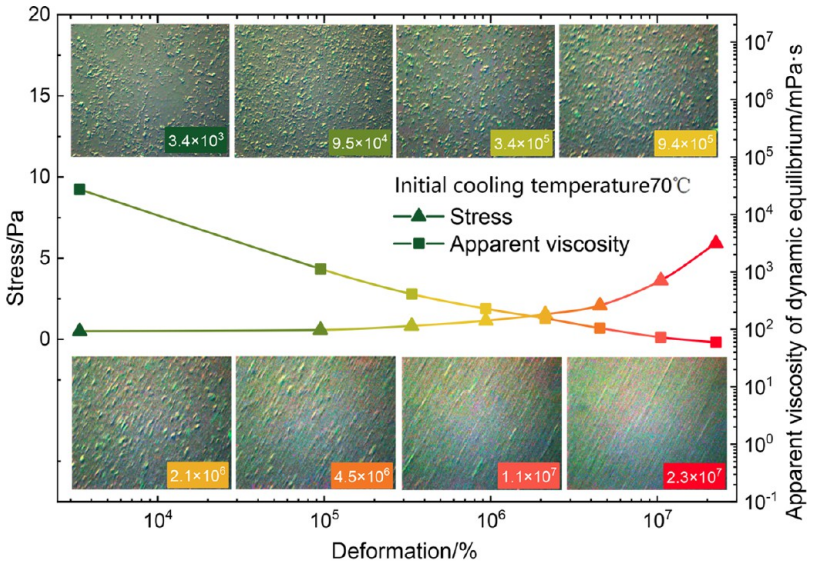

(a) Initial cooling temperature 70 ℃

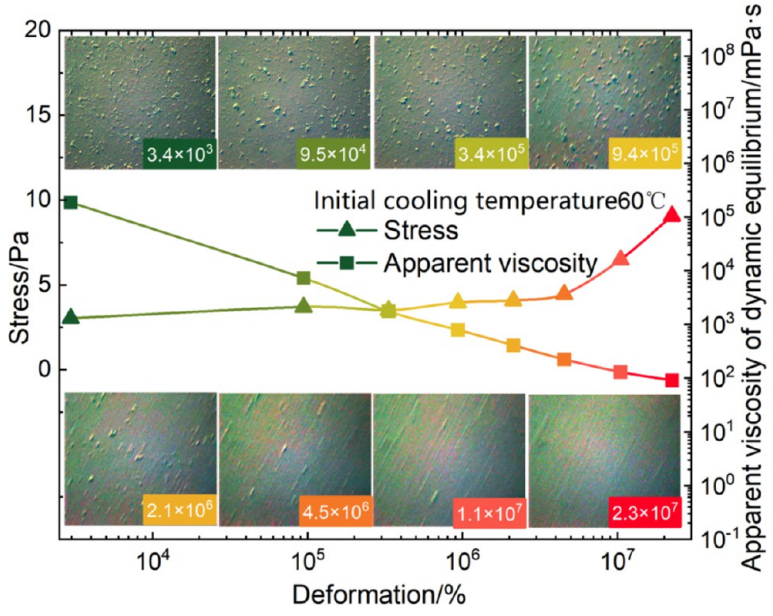

(b) Initial cooling temperature 60 °C

Figure 6. Simultaneous measurements of apparent viscosity, stress, and microstructure: (a) cooling from 70 and (b) 60 °C.

However, the melting point is not high enough to fully activate the asphalt, so Type II wax crystals form after cooling from the initial temperature of 60 °C, i.e., in the vicinity of the melting wax point.

3.2. In Situ Synchronized Rheo-optic Observations of Non-Newtonain Fluid Behavior of Waxy Crude Oil. Waxy crude oil is a non-Newtonain fluid below WAT, it has been studied, analyzed, and attributed to the rupture of the network structure of wax crystal flocculation and the arrangement of wax crystals under shearing and the orientation of the flow field. However, no direct observations have been made of changes in the microstructure during the structure breakage of waxy crude oil. The in situ rheo-optic measurement technology used in this paper provides a new means for the study of this problem and can identify the instantaneous dynamic response of wax crystals and their network structures to applied shear loads. The experimental procedures were as follows: a pretreated sample of M1 crude oil was heating from room temperature to different initial cooling temperatures (70 and 60 °C) and then cooled at a rate of 0.5 °C/min below the temperature of the onset of non-Newtonian viscosity (30 °C). After the sample was maintained at a constant temperature for 10 min, the thermostatic conditions were maintained while the sample was tested at shear rates of 0.01, 0.5, 2, 5, 10, 20, 50, and 100 s^{-1} in steps. Measurements lasted for 30 min at 0.01 and 0.5 s^{-1} each and 20 min at each of the other shear rates. Accordingly, the deformation at different shear rates are 3.4×10^3, 9.5×10^4, 3.4×10^5, 9.4×10^5, 2.1×10^6, 4.5×10^6, 1.1×10^7 and 2.3×10^7%. Measurements lasted for 30 min at 0.01 and 0.5 s^{-1} each and 20 min at each of the other shear rates. While obtaining the apparent viscosity and stress data of oil samples, the microstructure changes in wax crystals were observed in situ; the experimental results are as follows:

https://doi.org/10.1021/acsomega.2c01251
ACS Omega 2022, 7, 17948−17962

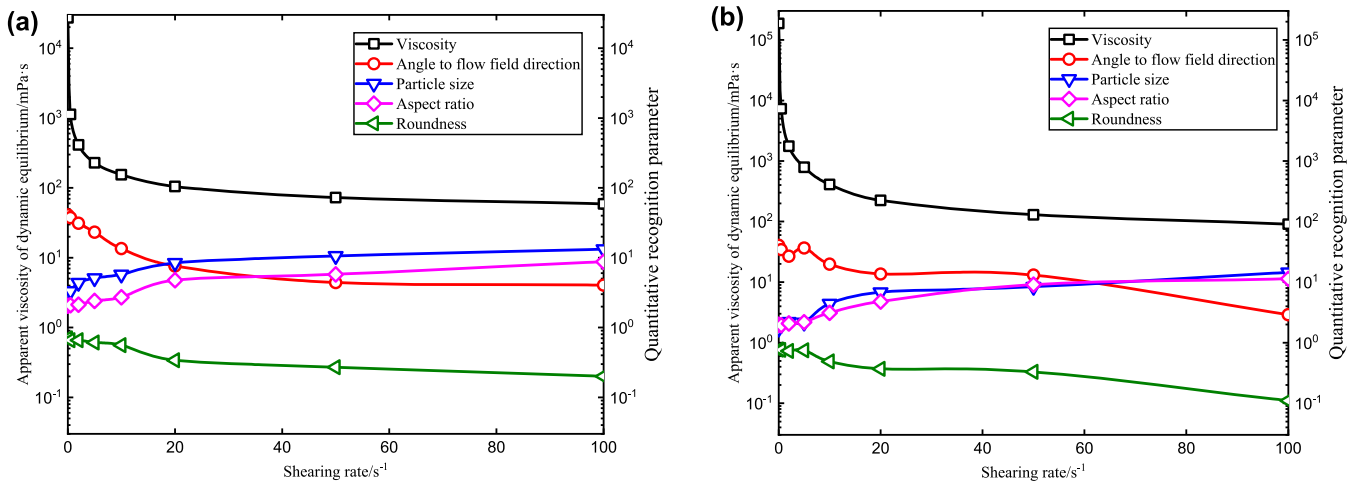

Figure 7. Microscopic parameters of wax crystals and the apparent viscosity vs shear rate: (a) cooling from 70 and (b) 60 °C.

Figure 6 shows that after the oil sample has undergone shearing, its apparent viscosity, stress, and deformation and the microstructure of the wax crystals have changed substantially. From a macroscopic perspective, the apparent viscosity of crude oil decreases greatly as the shear rate increases. From the microscopic point of view, the wax crystal aggregation structure changes with increasing shear rate, and its arrangement transitions from disordered to ordered and is increasingly aligned with the direction of the flow field. In terms of wax crystal morphology, the aspect ratio increases to a certain extent as the shear rate increases. Changes in the microstructure and morphology of wax crystals have effectively reduced the resistance of their convective field and the viscosity of the crude oil system. A closer comparison of the results in parts a and b of Figure 6 shows that the viscosity (186960 mPa·s) at the initial cooling temperature of 60 °C is appreciably greater than that at the initial cooling temperature of 70 °C (27184 mPa·s). With the increase in shear rate, the apparent viscosity decline is more apparent. Combined with the conclusions discussed in Section 3.1, these results show that different types of wax crystals can form inside crude oil with different initial cooling temperatures. These types of wax crystals have various forms, structures, interactions, and flocculation tendencies, which results in different adverse effects on macroscopic flow. To quantitatively analyze the relationship between the rheological of waxy crude oil and its microstructure, threshold segmentation and quantitative identification of wax crystals are carried out on the microscopic image in Figure 6. Four parameters (the average angle between the long axis direction of the wax crystal and the direction of the shear flow δ, the average aspect ratio of wax crystals A_r, the average roundness of wax crystals I, and the average particle size of the wax crystal D_P) are selected as quantitative parameters of the microstructure and morphology characteristics of the wax crystals. The parameters and the deformation γ of the crude oil are presented in the same graph as a function of shear rate. The results are shown in Figure 7.

The trends in the quantitative data in Figure 7 are basically consistent with the conclusions of the above analysis. When the shear rate increased from 0.01 to 100 s^{-1}, the value of wax crystal δ changed notably from 41.07° to 4.05° (initial cooling temperature 70 °C) and from 40.52° to 2.9° (initial cooling temperature 60 °C), indicating that the orientation of the wax crystal flow field was greatly enhanced. The wax crystal D_P value increased from 3.3 to 13.2 μm (70 °C) and from 1.71 to 14.45 μm (60 °C); these changes were related to the full extension of the wax crystal monomer structure under the action of the flow field and the shearing and destruction of the structure of the wax crystal aggregates or network. With increasing D_P, the value of wax crystal A_r increased with the shear rate, from 2.05 to 8.76 (70 °C) and from 1.98 to 11.38 (60 °C). Correspondingly, the wax crystal I value gradually decreased. Changes in the micromorphic forms of the wax crystals reduced their cross-sectional area in the direction of the flow field and the resistance of their convective field. Although the microscale parameters of wax crystals changed with increasing shear rate and contributed to the increasing in crude oil deformation, the correlations between various parameters and crude oil deformation differed. Using least-squares fitting, the microscale parameters δ, A_r, and D_P of wax crystals were used to establish a quantitative model with the γ and μ of crude oil. The results are shown in Table 2, and the relative deviation of the fitted results from the actual results is shown in Figure 8.

Table 2. Quantitative Model of the Microscopic Parameters of Wax Crystals and the Deformation of Crude Oil

initial cooling temperature (°C)	microscopic characteristic parameters of wax crystals	quantitative model	R^2
70	δ	$\gamma = 2 \times 10^7 e^{-0.129\delta}$	0.9817
	A_r	$\gamma = 49683e^{0.9635Ar}$	0.7593
	D_P	$\gamma = 28968e^{0.5959DP}$	0.8799
60	δ	$\gamma = 3 \times 10^7 e^{-0.14\delta}$	0.6836
	A_r	$\gamma = 165496e^{0.5129Ar}$	0.675
	D_P	$\gamma = 101326e^{0.5729DP}$	0.8195

As seen in Table 3, the strongest correlation is obtained between the wax crystal δ and the crude oil μ over the entire shear rate range (R^2 = 0.9555), followed by the correlation of A_r with μ (R^2 = 0.6703) and the correlation of D_P with μ (R^2 = 0.8112). In addition, the fitting deviation in Figure 8 shows that the microscopic parameters of wax crystals have different correlations with the crude oil viscosity in various shear rate ranges. The dominant factors affecting the reduction in crude oil viscosity at various shear rates differ. Although the correlation between δ and μ is strong over the range of

https://doi.org/10.1021/acsomega.2c01251
ACS Omega 2022, 7, 17948−17962

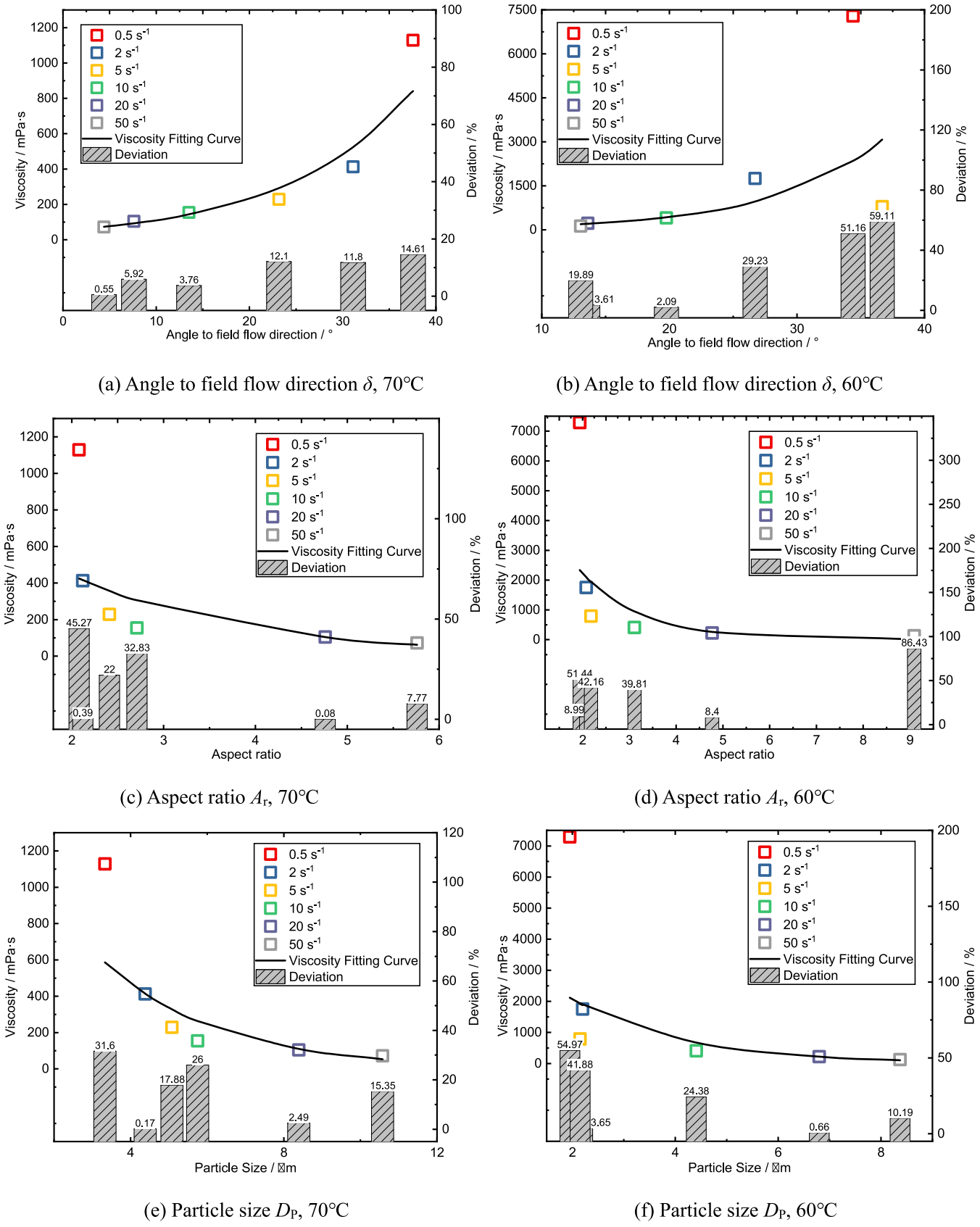

(a) Angle to field flow direction δ, 70°C

(b) Angle to field flow direction δ, 60°C

(c) Aspect ratio A_r, 70°C

(d) Aspect ratio A_r, 60°C

(e) Particle size D_P, 70°C

(f) Particle size D_P, 60°C

Figure 8. Regression analysis results for microstructure and rheological parameters at initial cooling temperatures of 70 and 60 °C: (a, b) δ; (c, d) A_r; (e, f) D_P.

shear rates, the relative deviation of the fit is greater when the shear rate is less than 5 s^{-1}. The contribution of δ to the decrease in μ in this range is not the most important factor, especially when the initial cooling temperature is 60 °C.

https://doi.org/10.1021/acsomega.2c01251
ACS Omega 2022, 7, 17948−17962

Table 3. Quantitative Model of the Microscopic Parameters of Wax Crystals and the Viscosity of Crude Oil

initial cooling temperature (°C)	microscopic characteristic parameters of wax crystals	quantitative model	R^2
70	δ	$\mu = 53.017e^{0.0736\delta}$	0.9555
	A_r	$\mu = 1261.9e^{-0.523Ar}$	0.6703
	D_P	$\mu = 1764.4e^{-0.331DP}$	0.8112
60	δ	$\mu = 42.212e^{0.1169\delta}$	0.6613
	A_r	$\mu = 10430e^{-0.771Ar}$	0.9646
	D_P	$\mu = 5265.2e^{-0.467DP}$	0.7573

However, when the shear rate exceeds 5 s^{-1}, this correlation increases sharply, and the relative deviation of fitting gradually reduces to 2.09% (10 s^{-1}), indicating that the orientation of the wax crystal convection field has a major influence on the rheological behavior only when the shear strength of the flow field exceeds a certain limit. In contrast, the correlation between the A_r and D_P of wax crystals and the μ of crude oil was greatly enhanced only after the shear rate exceeded 20 s^{-1}, and the relative deviation of their fitting decreased considerably, from more than 50% to approximately 10%. The changes in A_r and D_P with shear rate show that the micromorphology of wax crystals changes meaningfully only when the shear rate increases to a certain extent and has a considerable effect on the viscosity of crude oil. Combined with the above results, it is apparent that in different shear rate ranges, the dominant factors that determine the change in crude oil viscosity are indeed distinct.

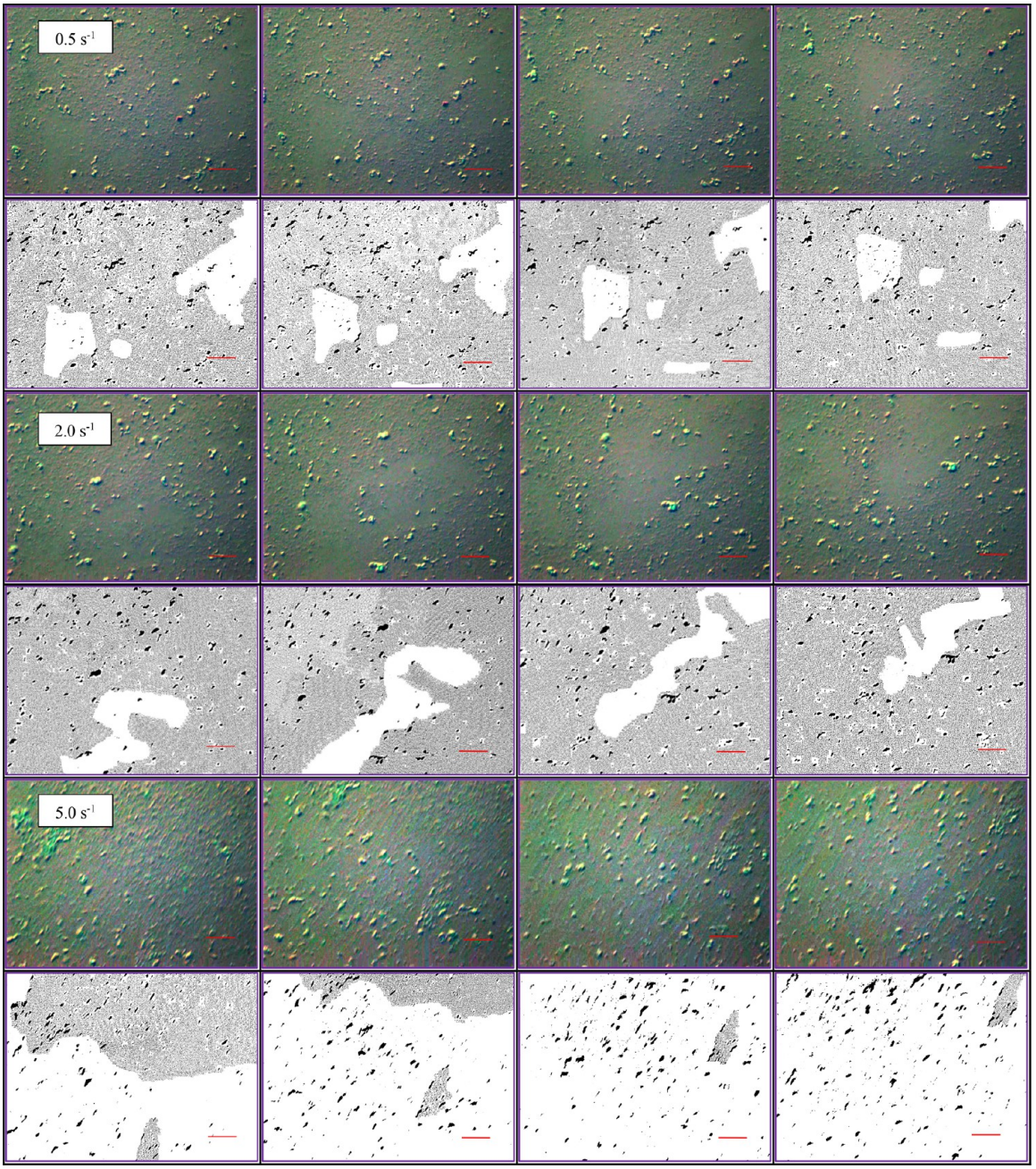

Figure 9. Changes in wax crystal structure and movement for different shear rates while cooling from 60 to 30 °C.

https://doi.org/10.1021/acsomega.2c01251
ACS Omega 2022, 7, 17948−17962

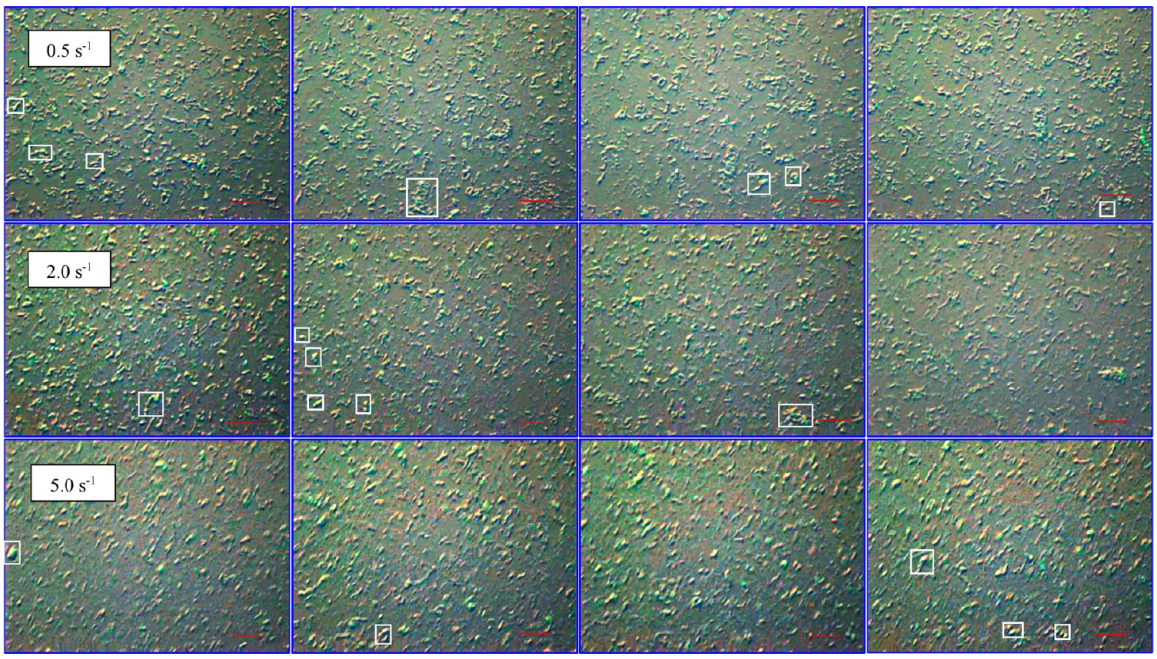

Figure 10. Sequences of images of wax crystal motion at different shear rates while cooling from 60 to 30 °C: internal 4 s under 0.5 s^{-1}, internal 2 s under 2.0 s^{-1}, and internal 0.66 s under 5.0 s^{-1}.

In addition, comparing the results of parts a and b of Figure 8 shows that there are statistically significant differences in the correlation results at different initial cooling temperatures. In Figure 8, the correlation between the wax crystal δ and the crude oil γ at the initial cooling temperature of 60 °C is much weaker than that at 70 °C. When the shear rate is less than 5 s^{-1}, the wax crystal δ fluctuates with increasing shear rate (Figure 7b), indicating that the enhancement of the orientation of the wax crystal flow field is not important, but the increasing in the deformation of crude oil in this range is more obvious at the initial cooling temperature of 60 °C. When the shear rate exceeds 10 s^{-1}, the orientation of the wax crystal flow field begins to increase notably at the initial temperature of 60 °C, and the correlation between the wax crystal δ and the crude oil γ strengthens. In addition, when the shear rate is less than 20 s^{-1}, the correlations between the wax crystal A_r and D_P at the initial temperature of 60 °C and the crude oil γ are much weaker than those at 70 °C. According to previous research, cooling from an initial temperature of 60 °C leads to the formation of Type II wax crystals, while cooling from 70 °C produces Type I wax crystals. The changes in the above microscopic parameters show that the destruction, orientation, and morphological changes in various types of wax crystal structures are different after shearing, and the effect on the rheological properties of the system is also different. Thus, more work was done to further explore the details of the changes in the microstructure of wax crystals caused by shearing, especially the dynamic response of wax crystal aggregates or network structures under additional shear load. The processes for changes in the microstructure of wax crystals at shear rates of 0.5, 2, and 5 s^{-1} and different initial cooling temperatures are visualized in the form of time series of microimages. To better reflect changes in wax crystal shape and structure, threshold segmentation of these images is displayed in Figure 9.

3.3. Dynamic Response of the Structure of Wax Crystal Networks under Shearing. In Figure 9, when the oil sample is cooled from 60 to 30 °C, it contains Type II wax crystals. Because wax crystals easily flocculate, a complete network structure forms. When the shear rate increases to 0.5 s^{-1}, the wax crystals in the field of view are still in the overall network flocculation state, and the wax crystals arrange along the flow field with the network structure. The large number of wax crystals in the flocculation network, which are closely spaced and undergo mutual interactions, shield the internal wax crystals of the network from the external flow field, hinder the orientation of the wax crystals along the flow field, increase the flow resistance of liquid hydrocarbons, and elevate the viscosity of the crude oil system. The corresponding sequence of motion images shows that although the shear at 0.5 s^{-1} does not destroy the wax crystal network structure, it causes some deformation of the network structure, which is indicated by the change in the shape of the blank area (without wax crystals) in the figure. The overall deformation of the wax crystal flocculation network structure changes the distances between the wax crystals and alters the overall shape of the network to reduce the resistance of the flow field, thus contributing to the reduction in the viscosity of the system. However, because the wax crystals are still bound in the flocculation network, the flexibility of individual motion is lost, and as a result, the angles between the long axes of the wax crystals and flow field are not greatly reduced (Figure 7b), and the wax crystals are not strongly oriented to the flow field.

As the shear rate increased from 0.5 to 2.0 s^{-1}, although the sequence of images shows that the flocculation network remained unbroken under the enhanced shear force, the overall deformation of the flocculation network was more significant, resulting in a notable increase in the blank area in the field of view. Because the deformation of the network structure increases, the interaction between the wax crystals changes, and the original stable connection weakens. The overall structural strength of the wax crystal flocculation network is reduced, and its overall shape changes by adapting to the flow

https://doi.org/10.1021/acsomega.2c01251
ACS Omega 2022, 7, 17948−17962

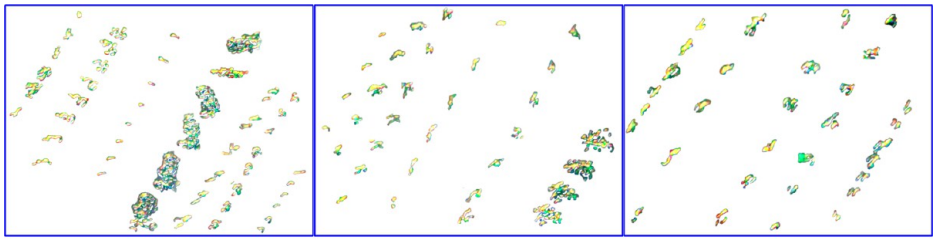

Figure 11. Images showing wax crystal motion at different shear rates: (a) 0.5 s^{-1}, (b) 2.0 s^{-1}, and (c) 5.0 s^{-1}.

field and reducing the flow resistance, thus reducing the viscosity of the system.

When the shear rate is further increased to 5.0 s^{-1}, the structure of the wax crystal flocculation network breaks, the large floc is gradually fractured into smaller flocs, and monomer wax crystals are released from the flocculation network. The released wax flocs and monomer particles begin to flow in the flow field under the shearing action, their separation increases, and their influence weakens, which greatly reduces the flow resistance of wax crystals in the system and further reduces the viscosity of the crude oil system. At the same time, the wax crystals are less restricted and move more freely, and they can better adapt to the flow field. It is also possible that when this shear rate is reached, the angle between the long axis and the flow field of the wax crystal in the field of view begins to decrease notably (Figure 7b), and the adaptability of the wax crystal motion convection field begins to increase.

When the tendency of flocculation between wax crystals is great and a strong flocculation network forms, the structural response of the network to external forces is directly related to the viscosity and other rheological parameters. A wax crystal network structure is observed, and the dynamic behavior under external force is observed by an in situ rheo-optic instrument, which helps to reveal the microscale mechanism of waxy crude oil rheological properties.

When the oil sample is reduced from the initial cooling temperature of 70 to 30 °C, the system contains mainly Type I wax crystals. The flocculation tendency of this kind of wax crystal is minor, and stable network structure does not form. Therefore, in this case, wax crystal do not respond to external forces as a whole network structure, but as monomer particles, and directly determines the macroscopic rheology of the system. Therefore, the microstructure changes of the wax crystals under shear rates of 0.5, 2, and 5 s^{-1} is visualized in the form of a time series of microimages, as shown in Figure 10, for cooling from 70 °C (Figure 6a).

3.4. Dynamic Behavior of Wax Particles under Shear.

As shown in Figure 10, when the oil sample is reduced from an initial cooling temperature of 70 to 30 °C, the wax crystals in the field of view do not form a flocculation network structure, and there are only a certain number of aggregates. In general, under these conditions, the wax crystal spacing is large, the interactions are weak, the clusters are small, and the structure is not strong. Because there is no wax flocculation network in the system, there is no deformation and destruction of network structure, resulting in a lower viscosity of crude oil than that at the initial cooling temperature of 60 °C, and at higher shear rates, the reduction in viscosity is smaller. To better illustrate the dynamic behavior of wax crystal particles and analyze their changes with shear rate, the next step was to select some representative wax crystal particles and aggregates (identified by the white border) in Figure 10, extract their microscale morphology and positions at different moments, and show them in Figure 11.

Figure 10 and 11 show that because there is no flocculation network structure, wax crystals have more freedom; mainly individual particles or clusters of wax crystals move in the flow field. When a wax crystal moves along the flow field, it also rotates within the microscale observation surface and spirals in three-dimensional space. This motion is related to the irregular shape of the wax crystals and their aggregates and it is caused by the imbalance of flow field torque on different parts of a crystal or an aggregate. Under shear at 0.5 s^{-1}, the wax crystals rotate and roll in the flow field, which increases the disturbance and resistance of the wax crystal convection field. Under these conditions, there is large-scale aggregate structure where the wax crystals are more closely associated and their interactions are strong, which resists shear without rupturing. As the shear rate increases to 2 s^{-1}, the number and size of wax crystal aggregates decrease. This indicates that shearing gradually destroys the wax crystal aggregate structure, which dissociates into smaller aggregates or individual wax crystals. The movement and orientation of these smaller aggregates and individual particles are enhanced in the direction of the flow field (Figure 7a), they undergo less rolling and rotating motion, wax crystal convection field disturbance and resistance are reduced, and the viscosity of the system decreases. When the shear rate was 5 s^{-1}, the number of wax crystal aggregates was much smaller, there were individual wax crystals throughout the oil, and wax particle orientation in the field was further enhanced (Figure 7a). Because of the simple structure of the individual wax crystals, the torque effect of the flow field balances, and there is much less rolling and rotating motion of the particles. In addition, the cross-sectional area of wax crystals perpendicular to the flow field is much smaller, the resistance of the convective field is smaller, and the viscosity of the crude oil lower. At the same time, the wax crystal morphology begins to be affected by the flow field and tends to stretch under the force of the flow field, which increases the aspect ratio (Figure 7a), thereby further reducing the resistance of the flow field. In summary, when a flocculation network structure does not form between wax crystals or after network structure is destroyed, there are changes in the structure, shape, aggregation and motion of wax crystals under the shearing action of the flow field. The dynamic behavior of wax crystal particles directly affects the flow of crude oil systems and determines the macroscopic rheological performance of the system; rheo-optic measurement technology provides a means of studying these physical phenomena.

The analysis of waxy crude oil microscale mechanism is of great importance for further exploration of the gel structure

https://doi.org/10.1021/acsomega.2c01251
ACS Omega 2022, 7, 17948−17962

Table 4. Wax Crystals Microstructure and Dynamic Behavior Evolution under Shearing

stage	shear rate range	microstructure and dynamic behavior evolution
I	0.01−0.5 s^{-1}	waxy crude oil system changes from static to dynamic, overcoming inertial effects.
II	0.5−5 s^{-1}	wax crystal flocculation network undergoes deformation, cracks, ruptures, breaks into wax crystal aggregates and individual wax crystals, and wax crystal aggregates break.
III	5−20 s^{-1}	wax crystal aggregation structure continues to break, the discrete monomer wax crystals or small aggregates orient along the flow field, and the wax crystal arrangement changes from disordered to ordered.
IV	20−100 s^{-1}	orientation of wax crystal movement along the flow field continues to increase, and the wax crystal morphology changes to be more suitable for the flow field.

and viscoelasticity of waxy crude oil. Combining the experimental results for different initial cooling temperatures and shear rates reported above, the dynamic behavior evolution of waxy crude oil can be divided into stages, and the dominant mechanism is unique in each stage. Because a wax crystal flocculation network structure formed at the initial temperature of 60 °C, the evolution process is more representative and more complete. Therefore, taking the initial temperature of 60 °C as an example, the wax crystals microstructure and dynamic behavior evolution under shearing is summarized in Table 4.

In general, the rheological properties of waxy crude oil is closely related to the dynamic response of the wax network flocculation structure, wax crystal aggregates and individual wax crystal particles under the effect of flow field shear. As the shear rate and deformation increasing, the viscosity of crude oil decreases, and the wax crystals microstructure changes continuously. Specifically, shearing first drives the waxy crude oil system from a static to a dynamic state to overcome its inertia, which reduces the system viscosity to the maximum extent (see Figure 10 (0.5 s^{-1}) and Figure 11a). Subsequently, the flocculation network structure formed by wax crystals gradually stretches and deforms under shear until cracks appear and expand through the structure (see Figure 10 (2.0 s^{-1}) and Figure 11b). Furthermore, the broken wax crystal aggregates and discrete monomer wax crystals orient along the flow field and undergo a transition from a disorderly arrangement to an orderly arrangement, and the aggregates may continue to break apart, which reduces the viscosity of the system (see Figure 10 (5.0 s^{-1}) and Figure 11c). Finally, discrete monomer wax crystals or dense small aggregates undergo small deformations under the action of the flow field, and changes in their morphology reduce the resistance of the flow field. This is the reason the system viscosity can decrease slightly when the shear rate increases to an extent.

4. CONCLUSIONS

Two types of wax crystals (Type I and Type II) with different mechanical properties were identified by in situ rheo-optic measurement technology. Rheological properties of waxy crude oil worsen with increasing proportion of Type II wax crystals. With the enhancement of shearing, wax crystal flocculation networks underwent deformation, then cracking and rupture, and then finally broke into wax crystal aggregates and individual wax crystals. During this process, the viscosity of the system was greatly reduced and the deformation was greatly. Waxy crude oil becomes a wax-gel and has a rheomalaxis behavior. Individual wax crystal particles migrated under shear, separated, and flowed along the field orientation. Their arrangement changed from disordered to ordered, and slight changes in morphology occurred under shear. The direction and order of wax crystal motion are characterized by the average angle between the long axes of the wax crystals and the direction of shear flow, δ. The microscale morphology of wax crystals is characterized by the wax crystal average aspect ratio, A_r, the average roundness of the wax crystal, I, and the average particle size of the wax crystal, D_p. Data for these characteristic parameters changed with shear rate. A model of the in situ rheological data was established. The mechanism of the macro-scale rheological properties of the system was further analyzed with correlation coefficients over a range of shear rates, and the microscale mechanism of waxy crude oil rheology was summarized.

■ ASSOCIATED CONTENT

Supporting Information

The Supporting Information is available free of charge at https://pubs.acs.org/doi/10.1021/acsomega.2c01251.

In situ synchronous rheo-optic measurement system, microscopic results by improved light source, and verification of experimental results (PDF)

■ AUTHOR INFORMATION

Corresponding Author

Jian Zhao − *Northeast Petroleum University, 163000 Daqing, Hei Longjiang, China; Young and Middle-aged Innovation Team of Northeast Petroleum University, 163000 Daqing, Hei Longjiang, China;* orcid.org/0000-0002-4592-5221; Email: zhaojian_nepu@163.com

Authors

Hang Dong − *Northeast Petroleum University, 163000 Daqing, Hei Longjiang, China; Young and Middle-aged Innovation Team of Northeast Petroleum University, 163000 Daqing, Hei Longjiang, China*

RunZe Ma − *Northeast Petroleum University, 163000 Daqing, Hei Longjiang, China*

Xiangrui Xi − *Northeast Petroleum University, 163000 Daqing, Hei Longjiang, China; Young and Middle-aged Innovation Team of Northeast Petroleum University, 163000 Daqing, Hei Longjiang, China*

Zhihua Wang − *Northeast Petroleum University, 163000 Daqing, Hei Longjiang, China; Young and Middle-aged Innovation Team of Northeast Petroleum University, 163000 Daqing, Hei Longjiang, China*

Complete contact information is available at: https://pubs.acs.org/10.1021/acsomega.2c01251

Notes

The authors declare no competing financial interest.

https://doi.org/10.1021/acsomega.2c01251
ACS Omega 2022, 7, 17948−17962

■ ACKNOWLEDGMENTS

This work was financially supported by the Heilongjiang Provincial Postdoctoral Science Foundation (LBH-Z18044) and the Northeast Petroleum University Youth Science Fund Project (2020QNL-03). The authors gratefully acknowledge the support from the young and middle-aged Innovation Team Program of Northeast Petroleum University (KYCXTD202101).

■ REFERENCES

(1) Li, C. *Crude Oil Rheology*; China University of Petroleum Press: DongYing, China, 2007; p 257.
(2) Zhang, J.-j.; Liu, X. Some advances in crude oil rheology and its application. *J. Cent. South Univ. Technol.* **2008**, *15*, 288−292.
(3) Magda, J. J.; El-Gendy, H.; Oh, K.; Deo, M. D.; Montesi, A.; Venkatesan, R. Time-Dependent Rheology of a Model Waxy Crude Oil with Relevance to Gelled Pipeline Restart. *Energy Fuels* **2009**, *23* (3−4), 1311−1315.
(4) Hasan, S. W.; Ghannam, M. T.; Esmail, N. Heavy crude oil viscosity reduction and rheology for pipeline transportation. *Fuel* **2010**, *89* (5), 1095−1100.
(5) Deshmukh, S.; Bharambe, D. P. Synthesis of polymeric pour point depressants for Nada crude oil (Gujarat, India) and its impact on oil rheology. *React. Fuel-Process. Technol.* **2008**, *89* (3), 227−233.
(6) Deka, B.; Sharma, R.; Mandal, A.; Mahto, V. Synthesis and evaluation of oleic acid based polymeric additive as pour point depressant to improve flow properties of Indian waxy crude oil. *J. Pet. Sci. Eng.* **2018**, *170*, 105−111.
(7) Zhang, J. J.; Yu, B.; Li, H. Y.; Huang, Q. Y. Advances in rheology and flow assurance studies of waxy crude. *Pet. Sci.* **2013**, *10* (4), 538−547.
(8) Raju, G. A.; Shirodkar, S.; Marathe, S. R. NEXUS BETWEEN CRUDE OIL, EXCHANGE RATE AND STOCK MARKET RETURNS: AN EMPIRICAL EVIDENCE FROM INDIAN CONTEXT. *International Journal of Energy Economics and Policy* **2021**, *11* (3), 170−175.
(9) Brown, C. E. *World Primary Energy Overview*; Springer: Berlin and Heidelberg, Germany, 2002.
(10) Visintin, R. F. G.; Lapasin, R.; Vignati, E.; D'Antona, P.; Lockhart, T. P. Rheological behavior and structural interpretation of waxy crude oil gels. *Langmuir* **2005**, *21* (14), 6240−6249.
(11) Quan, Z. A Discussion on Crude Oil Rheology and Petrochemistry. *Oil Gas Storage* **1996**, *10*, 1−6.
(12) Matveenko, V. N.; Kirsanov, E. A.; Remizov, S. V. Rheology of highly paraffinaceous crude oil. *Colloids Surf., A* **1995**, *101* (1), 1−7.
(13) Riehm, D. A.; Rokke, D. J.; Mccormick, A. V. Water-in-Oil Microstructures Formed by Marine Oil Dispersants in a Model Crude Oil. *Langmuir* **2016**, *32*, 3954−3962.
(14) Sokolovic, R.; Sokolovic, S.; Mihajlovic; Gelei, T.; Pekaric, N.; Sevic, S. a. Effect of Pulsed Electromagnetic Field on Crude Oil Rheology. *Ind. Eng. Chem. Res.* **1998**, *37* (12), 4828−4834.
(15) Goncalves, J. L.; Bombard, A.; Soares, D.; Carvalho, R.; Nascimento, A.; Silva, M. R.; Alcantara, G. B.; Pelegrini, F.; Vieira, E. D.; Pirota, K. R.; et al. Study of the Factors Responsible for the Rheology Change of a Brazilian Crude Oil under Magnetic Fields. *Energy Fuels* **2011**, *25* (8), 3537−3543.
(16) Luo, T. Research on Waxy Crude Oil Rheology. *Oil & Gas Storage and Transportation* **1989**, *8*, 7.
(17) Kane, M.; Djabourov, M.; Volle, J. L. Rheology and structure of waxy crude oils in quiescent and under shearing conditions. *Fuel* **2004**, *83* (11−12), 1591−1605.
(18) Lei, Q.; Zhang, F.; Guan, B.; Liu, G.; Zhu, Z.; et al. Influence of shear on rheology of the crude oil treated by flow improver. *Energy Rep.* **2019**, *5*, 1156−1162.
(19) Gao, P.; Zhang, J. J.; Hou, L.; Wang, H. F. Relationship between waxy crude viscosities and wax crystal microstructure. *J. Cent. South Univ. Technol.* **2008**, *15*, 406−410.
(20) Navarro, F. J.; Partal, P.; Martínez-Boza, F.; Gallegos, C.; Bordado, J.; Diogo, A. Rheology and microstructure of MDI−PEG reactive prepolymer-modified bitumen. *Mech. Time-Depend. Mater.* **2007**, *10* (4), 347−359.
(21) Yang, F.; Li, C.; Wang, D. Studies on the Structural Characteristics of Gelled Waxy Crude Oils Based on Scaling Model. *Energy Fuels* **2013**, *27* (3), 1307−1313.
(22) Muriel, D. F.; Gupta, S.; Katz, J. Effect of Oil Properties on the Generation of Nano-Aerosols During Bubble Bursting Through Crude Oil-Dispersant Slicks. *Langmuir* **2021**, *37* (45), 13365−13378.
(23) Venkatesan, R.; Nagarajan, N. R.; Paso, K.; Yi, Y. B.; Sastry, A. M.; Fogler, H. S. The strength of paraffin gels formed tinder static and flow conditions. *Chem. Eng. Sci.* **2005**, *60* (13), 3587−3598.
(24) Bolintineanu, D. S.; Grest, G. S.; Lechman, J. B.; Pierce, F.; Plimpton, S. J.; Schunk, P. R. Particle dynamics modeling methods for colloid suspensions. *Computational Particle Mechanics* **2014**, *1* (3), 321−356.
(25) Dong, H.; Zhao, J.; Wei, L.; Liu, Y.; Li, Y. Effect of Initial Cooling Temperature on Structural Behaviors of Gelled Waxy Crude Oil and Microscopic Mechanism Investigation. *Energy Fuels* **2020**, *34* (12), 15782−15801.
(26) Yi, S.; Zhang, J. Relationship between Waxy Crude Oil Composition and Change in the Morphology and Structure of Wax Crystals Induced by Pour-Point-Depressant Beneficiation. *Energy Fuels* **2011**, *25* (4), 1686−1696.
(27) Jiaqiang, J. Study of Waxy Crude oils Structure Depression Mechanism. *J. Southwest Pet. Inst.* **2004**, 71−74.
(28) Geri, M.; Venkatesan, R.; Sambath, K.; Mckinley, G. H. Thermokinematic memory and the thixotropic elasto-viscoplasticity of waxy crude oils. *J. Rheol.* **2017**, *61* (3), 427−454.
(29) Eke, W. I.; Kyei, S. K.; Ajienka, J.; Akaranta, O. Effect of biobased flow improver on the microscopic and lowtemperature flow properties of waxy crude oil. *J. Pet. Explor. Prod. Technol.* **2021**, *11*, 711.
(30) Song, S.; Shi, B.; Yu, W.; et al. A new methane hydrate decomposition model considering intrinsic kinetics and mass transfer. *Chem. Eng. J.* **2019**, *361*, 1264−1284.
(31) Zhang, F. X.; Fang, L.; Nie, Z. G.; Zhang, X. D. Preparation and mechanism of a pour point depressant for high pour point crude oil. *Acta Pet. Sin., Pet. Process. Sect.* **2009**, *25* (6), 801−806.
(32) Huang, H. R.; Wang, W.; Peng, Z. H.; Yang, F.; Zhang, X. F.; Ding, Y. F.; Li, K.; Wang, C. S.; Gan, D. Y.; Gong, J. Magnetic Organic-Inorganic Nanohybrid for Efficient Modification of Paraffin Hydrocarbon Crystallization in Model Oil. *Langmuir* **2020**, *36* (2), 591−599.
(33) Hong, Z.; Shen, B. Study of crude oil doped with pour point depressant. *Chemistry* **2007**, *70* (1), 73−76.
(34) Yao, B.; Li, C. X.; Yang, F.; Zhang, Y.; Xiao, Z. Q.; Sun, G. Y. Structural properties of gelled Changqing waxy crude oil benefitted with nanocomposite pour point depressant. *Fuel* **2016**, *184*, 544−554.
(35) Peng, Z. H.; Wang, W.; Cheng, L.; Yu, W. J.; Li, K.; Liu, Y. M.; Wang, M. X.; Xiao, F.; Huang, H. R.; Liu, Y.; Ma, Q. L.; Shi, B. H.; Gong, J. Effect of the Ethylene Vinyl Acetate Copolymer on the Induction of Cyclopentane Hydrate in a Water-in-Waxy Oil Emulsion System. *Langmuir* **2021**, *37* (45), 13225−13234.
(36) Zhang, J.; Guan, J.; Song, N.; Zhou, J.; Cheng, Y. INFLUENCE OF POUR POINT DEPRESSANT ON WAX CRYSTAL MORPHOLOGY OF CRUDE OIL. *Acta Pet. Sin., Pet. Process. Sect.* **2010**, *2010* (5), 1−51.
(37) Chen, C.; Zhang, J.; Xie, Y.; Huang, Q.; Li, H.; et al. An Investigation to the Mechanism of the Electrorheological Behaviors of Waxy Oils. *Chem. Eng. Sci.* **2021**, *239*, 116646.
(38) Li, H.; Li, Z.; Xie, Y.; Guo, W.; Zhang, J.; et al. Impacts of Shear and Thermal Histories on the Stability of Waxy Crude Oil Flowability Improvement by Electric Treatments. *J. Pet. Sci. Eng.* **2021**, *204*, 108764.
(39) Huang, Q.; Li, H. Y.; Xie, Y. W.; Ding, Y. F.; Zhuang, Y.; Chen, C. H.; Han, S. P.; Zhang, J. J. Electrorheological behaviors of waxy crude oil gel. *J. Rheol.* **2021**, *65* (2), 103−112.

https://doi.org/10.1021/acsomega.2c01251
ACS Omega 2022, 7, 17948−17962

(40) Legnani, A.; Santos, T. G. M.; Andrade, D. E. V.; Negrão, C. O. R. Waxy oils: deformation-dependent materials. *J. Non-Newtonian Fluid Mech.* **2020**, *285*, 104378.
(41) Rodriguez-Fabia, S.; Lopez Fyllingsnes, R.; Winter-Hjelm, N.; Norrman, J.; Paso, K. G. Influence of measuring geometry on rheomalaxis of macrocrystalline wax−oil gels: alteration of breakage mechanism from adhesive to cohesive. *Energy Fuels* **2019**, 33 (2), 654.
(42) Tikariha, L.; Kumar, L. Pressure propagation and flow restart in a pipeline filled with a gas pocket separated rheomalaxis elasto-viscoplastic waxy gel. *J. Non-Newtonian Fluid Mech.* **2021**, *294*, 104582.
(43) Qicheng, S.; Gguangqian, W. *An introduction to mechanics of granular materials*; Science Press: 2009.
(44) Qicheng, S.; Meiying, H.; Feng, J. *Particulate matter physics and mechanics*; Science Press: 2011.
(45) Cheng, X.; McCoy, J. H.; Israelachvili, J. N.; Cohen, I. Imaging the Microscopic Structure of Shear Thinning and Thickening Colloidal Suspensions. *Science.* **2011**, *333* (6047), 1276−1279.
(46) Dupire, J.; Socol, M.; Viallat, A. Full dynamics of a red blood cell in shear flow. *Proc. Natl. Acad. Sci. U. S. A.* **2012**, *109* (51), 20808−20813.
(47) Huang, Y.; Ding, W.; Hongguang, L. I. Haze removal method for UAV reconnaissance images based on image enhancement. *J. Beijing Univ. Aeronaut. Astronaut.* **2017**, *43* (3), 592−601.
(48) Khan, A.; Majumdar, D. De-Noising of Binary Image Using Accelerated Local Median-Filtering Approach. *Advances in Data Mining and Database Management* **2019**, 164−185.

https://doi.org/10.1021/acsomega.2c01251
ACS Omega 2022, 7, 17948−17962